



## Crystallization of a basal magma ocean recorded by Helium and Neon

Nicolas Coltice <sup>a,\*</sup>, Manuel Moreira <sup>b,d</sup>, John Hernlund <sup>c</sup>, Stéphane Labrosse <sup>a,d</sup>

<sup>a</sup> Laboratoire de Géologie de Lyon, Terre, Planètes, Environnement; Université Lyon 1; Ecole Normale Supérieure de Lyon; Université de Lyon, France

<sup>b</sup> Institut de Physique du Globe de Paris, France

<sup>c</sup> Department of Earth Sciences, University of California Berkeley, USA

<sup>d</sup> Institut Universitaire de France, France

### ARTICLE INFO

#### Article history:

Received 12 December 2010

Received in revised form 23 May 2011

Accepted 24 May 2011

Available online 16 June 2011

Editor: R.W. Carlson

#### Keywords:

mantle dynamics

noble gasses

early Earth

geochemistry

geophysics

### ABSTRACT

Interpretation of the noble gas isotopic signature in hotspots is still controversial. It suggests that relatively primitive material remains untapped in the deepest mantle, even while mantle convection and sub-surface melting efficiently erase primordial heterogeneities. A recent model suggests that significant differentiation and fractionation affects the deepest mantle following the formation of a dense basal magma ocean (BMO) right after core segregation (Labrosse et al., 2007). Here we explore the consequences of the crystallization of a BMO for the noble gas evolution of the mantle. The crystals extracted from a BMO upon cooling generate dense chemical piles at the base of the mantle. We show that if the solid–melt partition coefficients of He and Ne are  $>0.01$  at high pressure and temperature, He and Ne isotopic ratios in pile cumulates can be pristine like. Hence, the entrainment of modest amounts of BMO cumulate in mantle plumes ( $<10\%$ ) potentially explains the primitive-like He and Ne signatures in hotspots. Because pile material can be depleted in refractory elements while simultaneously enriched in noble gasses, our model forms a viable hypothesis to explain the complex relationship between He and refractory isotopic systems in Earth's interior.

© 2011 Elsevier B.V. All rights reserved.

### 1. Introduction

The isotopic signatures of oceanic island basalts (OIBs) are a cornerstone for building models of the evolution of Earth's mantle through time (Hofmann, 1997 for a classic review). Lithophile isotopic systems are particularly useful, since most of them document fractionation and segregation upon melting, and hence crust–mantle differentiation. In the 1980s, Sr, Nd and Pb isotopes were used to show that the mantle sources of many oceanic islands contain recycled crustal components (e.g. Allègre et al., 1987; Dupré and Allègre, 1983; Hart, 1988; Storey et al., 1988). Improvements in geochemical analytical methods allowed higher precision studies on isotopic systems such as Re/Os or Lu/Hf. These new data confirmed the presence of recycled crustal components from deep oceanic crust to pelagic sediments in the source of most hotspot basalts, with Hawaii and Iceland being the most popular targets (Blichert-Toft et al., 1999; Hauri and Hart, 1993).

Helium and Neon both have U and Th parentage:  $^4\text{He}$  and  $^{21}\text{Ne}$  are radiogenic and nucleogenic isotopes, respectively, produced within the radioactive chains of  $^{235,238}\text{U}$  and  $^{232}\text{Th}$ . Other isotopes are stable and almost non-radiogenic/nucleogenic (e.g. primordial):  $^3\text{He}$  and

$^{20,22}\text{Ne}$ . Variability in  $^4\text{He}/^3\text{He}$  and  $^{21}\text{Ne}/^{22}\text{Ne}$  is caused by ancient degassing and extraction/recycling of U and Th. Low  $^4\text{He}/^3\text{He}$  and  $^{21}\text{Ne}/^{22}\text{Ne}$  isotopic ratios have been measured in many OIBs (Honda et al., 1991; Moreira et al., 1995; Moreira et al., 2001; Moreira et al., 2004; Poreda and Farley, 1992; Tieloff et al., 2000; Yokochi and Marty, 2004). These signatures have not been observed in crustal rocks, perhaps owing to release of noble gasses into the atmosphere upon formation of the crust.

Models are then needed to reconcile the simultaneous occurrence of primitive-like isotopic ratios of noble gasses and ubiquitous recycling of crustal components in mantle plumes. The proposed alternative was that the source of these OIBs (a) sample a deep pristine and little degassed reservoir (Allègre et al., 1987) or (b) contain old recycled lithospheric mantle depleted in radioactive elements (Coltice and Ricard, 1999). In the pristine model, the primitive mantle has to be intrinsically denser to be preserved from convective mixing. However, there is no evidence for any significant major element difference between primitive and depleted mantle that would lead to such a density difference. Moreover, the refractory isotope ratios of primitive-like OIBs are almost similar to those of the depleted bulk mantle, which is the source of mid oceanic ridge basalts. An argument against the recycling model was proposed by Kurz et al. (2009) based on Neon isotopes in Galapagos samples. In order to explain observed non-nucleogenic  $^{21}\text{Ne}/^{22}\text{Ne}$  ratios by a residual component, a depletion age of 4.4 Ga is implied, which is difficult to justify. Thus both the pristine reservoir and crustal recycling models

\* Corresponding author.

E-mail address: [coltice@univ-lyon1.fr](mailto:coltice@univ-lyon1.fr) (N. Coltice).

have shortcomings, prohibiting the development of any consensus regarding the origin of noble gas signatures in OIBs.

Recently a new class of models has emerged, in which early differentiation generated a fractionated enriched reservoir, for instance subducted early crust, that would have sequestered a significant fraction of incompatible element in the deepest mantle (Boyet and Carlson, 2006; Tolstikhin and Hofmann, 2005). The peculiar noble gas signature of some OIBs would be explained by sampling of the early reservoir by mantle plumes (Jackson et al., 2010). Within this family of models, Labrosse et al. (2007) proposed that early differentiation took place in the deep mantle with the formation of a basal magma ocean (BMO). The presence of dense material above the core–mantle boundary in the present-day Earth has been inferred in ultralow seismic velocity zones (ULVZ) at the core–mantle boundary, which may be close to the solidus or partially molten (Rost et al., 2005; Williams and Garnero, 1996). Because the core has been cooling for more than 3.2 Ga as evidenced by the persistence of a geomagnetic field (Labrosse, 2003; Tarduno et al., 2007), these ULVZ patches lying above the core should naturally be remnants of a larger magma body formed early in Earth's history (Labrosse et al., 2007). It has been proposed that the entrainment of the material crystallized from the cooling BMO could explain the signature of primitive-like noble gases in mantle plumes. Contrarily to Boyet and Carlson (2006) and Tolstikhin and Hofmann (2005), it is not the entrainment of the enriched reservoir that would occur, but that of the cumulates (i.e., the crystals extracted as the melt crystallizes). Here we explore this scenario further, and predict the required Helium and Neon partitioning upon deep melting/crystallization to simultaneously explain depleted lithophile characteristics along with primitive-like noble gas signatures in OIB.

## 2. Influence of a basal magma ocean on mantle heterogeneity

The slow cooling of the BMO induces its progressive fractional crystallization. Because of the large Grüneisen parameter of the magma (Mosenfelder et al., 2007; Mosenfelder et al., 2009), the isentropic temperature gradient in the melt may be larger than the gradient of the liquidus due to a small molar volume difference between melt and solid at high pressure (Fig. 1). Under these

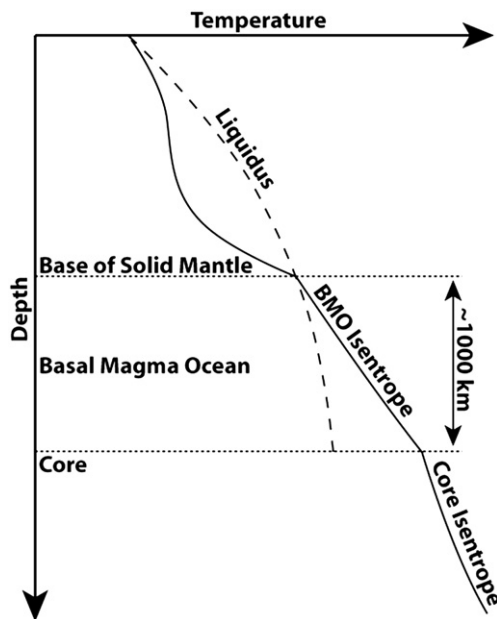


Fig. 1. Schematic temperature profile in the mantle, basal magma ocean and the core of the Earth. The liquidus is represented to discuss the nature and fate of crystals formed through the cooling of the basal magma ocean.

circumstances, crystals would form at the top of the melt layer. The phase diagram of the deep mantle is poorly known but since the starting composition of the BMO is very similar to that of the mantle (Labrosse et al., 2007) the liquidus phase is very likely to be (Mg, Fe) SiO<sub>3</sub> perovskite (Fiquet et al., 2010). Hence, crystals are Mg rich and consequently less dense than the melt. This results in a fractional crystallization evolution, with solid cumulates rising upward to the top of the BMO and subsequently becoming accessible to entrainment in convection currents in the solid mantle (see Fig. 2A). As crystallization advances, the residual melt becomes richer and richer in iron, and so do the crystals that subsequently form. Eventually, cumulates become dense enough to be gravitationally stable against immediate entrainment by mantle convection and accumulate as thermo-chemical piles above the BMO as proposed in Fig. 2B. To resist entrainment, the intrinsic density of the crystal must exceed about 2.5% in the deepest mantle (Davaille, 1999). This scenario is consistent with the presence of broad low shear wave anomalies extending several hundred kilometers above the core–mantle boundary, which represent a ubiquitous and robust feature in seismic tomographic models (Bolton and Masters, 2001; Hernlund and Houser, 2008; Karason and van der Hilst, 2001; McNamara and Zhong, 2005; Megnin and Romanowicz, 2000).

The deep and dense piles which form by accumulation of dense cumulates above the BMO are the only possible vector to transfer the chemical signal of the BMO to the surface because the liquid is itself relatively dense and is expected to have a very low viscosity (Karki and Stixrude, 2010). The crystals from the BMO can be entrained viscously by deep mantle plumes that start from the edges of piles which are the hottest regions of piles and location of BMO melt remnants (McNamara et al., 2010). Depending on the partitioning behavior of noble gases at high pressure and temperature, piles can have a high concentration of noble gases. Indeed, the crystals form out of the BMO, protected from subsurface degassing which has stripped most of the volatiles from the convecting mantle (Allègre et al., 1987).

## 3. Dynamical model of rare gas evolution

Our goal is to compute the rare gas evolution in the piles formed out of the BMO. The model is developed on the basis of previous work proposing a model of BMO evolution (Labrosse et al., 2007). The considered reservoirs are: the bulk mantle which is the whole

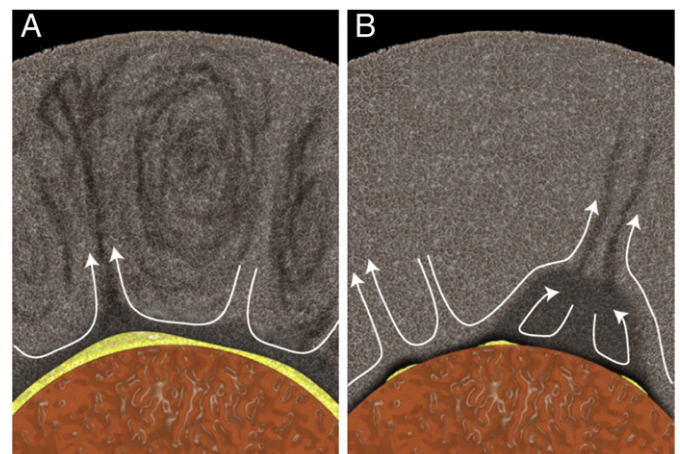


Fig. 2. Schematic dynamical evolution of the deep mantle. While the BMO crystallizes following mantle cooling, the crystals become richer in Fe. In a first stage (A) the crystals can be easily entrained and mixed back in the bulk mantle. In a later stage (B), the crystals are dense enough to form stable piles resisting convective entrainment. Today only plumes anchored on piles can modestly sample them.

convective mantle above the piles and BMO, the piles, that represent the mixing of the crystals of different ages, that remain at a given time at the base of the mantle, and the BMO which is the molten fraction in the deepest mantle that crystallizes through Earth cooling.

### 3.1. Pile growth

Thermal evolution models suggest that the mass of the BMO decays approximately exponentially with time (Labrosse et al., 2007). Hence the mass of crystals formed out of it grows like

$$M_c = M_0(1 - e^{-t/\tau}) \quad (1)$$

where  $M_0$  is the initial mass of the BMO and  $\tau$  its decay time typically around 900 Gy. The dense cumulates forming from the BMO begin to stabilize against entrainment and accumulate as dense piles at a time  $t_p$ , which is difficult to evaluate. To be stable, the crystals have to be dense enough and hence sufficiently rich in iron. Mg–Fe fractionation is expected to be significant after 50% crystallization. At the same time, the entrained crystals carry a signal of deep fractionation that should be observed in surface rocks. Such evidence is particularly difficult to observe and we can only propose putative constraints. Deep fractionation caused by the BMO would produce  $^{142}\text{Nd}$  anomalies in the residual crystals. No anomaly has been observed in rocks younger than 3.5 Ga old (Bennett et al., 2007), which suggests that limited amounts of pile material are sampled since the meso-archean. Pile stabilization is then probably reached no later than 3.0 Ga, which implies 80% of BMO crystallization (Fig. 2). Later times of stabilization would not have the potential to generate a sufficient mass of crystals to explain the observed volume of anomalous material in the deep mantle (Hernlund and Houser, 2008).

While they grow, piles also lose material through entrainment by plumes. Since there is no physical framework available to estimate pile entrainment, we chose a relatively simple model relying on two principles: (a) entrainment is proportional to the mass of existing piles and (b) entrainment decays with time as crystallizing material becomes more dense. Hence, the evolution of  $M_p$ , the mass of piles, is described as follows

$$M_p(t > t_p) = M_0(1 - e^{-t/\tau}) - M_0(1 - e^{-t_p/\tau})e^{-(t-t_p)/\sigma} \quad (2)$$

where  $\sigma$  is a decay time that can be constrained using seismological estimates of the present-day mass of piles (around 2% of mantle volume following Hernlund and Houser, 2008). The time of stabilization of pile material is used to estimate  $\sigma$  and taking 3.5 Ga leads to a value close to 12 Ga, which implies a rate of entrainment that decays very slowly.

### 3.2. Conservation of the chemical species

The chemical concentration  $C_p^i$  for the isotope  $i$  of the piles evolves through (a) the influx  $F_{m \rightarrow p}$  from crystals extracted out of the BMO, (b) radiogenic ingrowth from the decay of isotope  $j$  of constant  $\lambda^j$ , (c) an outflux of entrainment  $F_{p \rightarrow s}$  to the convecting mantle and (d) radioactive decay of constant  $\lambda^i$ :

$$\frac{dM_p C_p^i}{dt} = F_{m \rightarrow p} - F_{p \rightarrow s} + \lambda^j M_p C_p^j - \lambda^i M_p C_p^i. \quad (3)$$

The concentration of piles is an average here, although the situation could be more complex when the BMO becomes small enough and not continuous anymore. In this case, portions of BMO and corresponding piles should be treated separately. However, such scenario is difficult to model since a 3D thermal evolution of the mantle should be known. Hence, we focus on the zeroth order

chemical evolution. The flux of elements from the BMO to the piles is given by

$$F_{m \rightarrow p} = -D^i \frac{dM_m C_m^i}{dt} \quad (4)$$

where  $M_m$  and  $C_m$  are the mass and composition of the BMO given in Labrosse et al. (2007).  $D^i$  is the partition coefficient of the considered element, defined at equilibrium as

$$D^i = \frac{C_{crystal}^i}{C_{melt}^i}.$$

The flux of entrainment  $F_{p \rightarrow s}$  is obtained from derivation of the second term of the right hand side of Eq. 2:

$$F_{p \rightarrow s} = M_0 e^{t_p/\sigma} \left\{ \left( \frac{1}{\tau} + \frac{1}{\sigma} \right) e^{-t(\frac{1}{\tau} + \frac{1}{\sigma})} - \frac{1}{\sigma} e^{-t/\sigma} \right\} C_p^i. \quad (5)$$

Combining these equations gives

$$\frac{dC_p^i}{dt} = \frac{1}{M_p} \frac{dM_m}{dt} \{ C_p^i - D^i C_m^i \} + \lambda^j C_p^j - \lambda^i C_p^i. \quad (6)$$

The evolution of  $M_m$  and  $C_m$  is given as analytical expressions in Labrosse et al. (2007). However,  $C_p$  can only be obtained numerically solving for Eq.2 and Eq.6. In this study we use a 4th order Runge–Kutta method.

### 3.3. Variables of the model

The volatile content of the Earth after accretion and early differentiation is far from being known, mostly because the nature and origin of the parent bodies and the physical processes involved from gas incorporation to impact degassing are still open questions. Indeed, Earth is depleted in moderately volatile elements such as K or Rb. It might then be suggested that Earth is very depleted in highly volatile elements such as rare gasses (Albarède, 2009). However, recent studies have proposed that solar wind implantation during planetary formation could have brought enough rare gasses in parent bodies without invoking any late veneer of volatile-rich material. This is based on the Neon and Argon isotopic signatures of mantle-derived rocks that reflect ion implantation from solar wind (Raquin and Moreira, 2009; Trielloff et al., 2000; Trielloff et al., 2002; Trielloff and Kunz, 2005). In such a scenario, Helium and Neon isotopic ratios are close to the solar isotopic ratios (Black, 1971) although fractionated during the process of implantation (Grimberg et al., 2006; Raquin and Moreira, 2009). The starting Neon isotopic composition is similar to the so-called Neon B isotopic ratio, whereas the Helium isotopic ratio can be taken as the solar wind ratio i.e. 2500 (Wieler, 2002). The initial  $^3\text{He}/^{22}\text{Ne}$  ratio is taken here to be 1, similar to extraterrestrial samples having a Neon B signature. This is also in agreement with the samples having the most primitive Neon on Earth and that are not significantly degassed (e.g. Galapagos; Kurz et al., 2009; Raquin and Moreira, 2009).

The only remaining variable that needs to be specified is the initial concentration of  $^3\text{He}$  in the early Earth. The presumed parent bodies (i.e., chondrites) exhibit a variability over several orders of magnitude. In addition, the degassing experienced by the parent bodies during early planetary formation is not well constrained. The lower bound of  $^3\text{He}$  content in the primitive Earth is larger than that of the present day bulk mantle, the latter of which is already degassed. This value is estimated to be around  $1.5 \times 10^{-12} \text{ mol kg}^{-1}$  (Ballentine et al., 2005; Coltice and Ricard, 2002) and should be much lower than the initial concentration prior to surface outgassing. Hence we vary the initial concentration of  $^3\text{He}$  in the mantle from  $1.5 \times 10^{-11} \text{ mol kg}^{-1}$  (10 times that of the bulk mantle today) to  $1.5 \times 10^{-9} \text{ mol kg}^{-1}$  (1000 times that of the bulk mantle

today) as suggested by models of degassing evolution (Coltice et al., 2009). Table 1 gives a summary of the parameters used in our model.

#### 4. Results

In this section, we investigate how pile material can contribute to the isotopic variations observed in OIBs, determining values for HP–HT (high pressure–high temperature) partition coefficients of Helium and Neon. Considerable progress has been made to measure partitioning for He and Ne at low pressure (Brooker et al., 2003; Heber et al., 2007; Parman et al., 2005) and it is suggested that noble gases are moderately to very incompatible with partition coefficients lower than 0.01. It has been suggested on a theoretical basis that noble gases could become more compatible with increasing pressure (Wood and Blundy, 2001). However, other experiments seem to contradict this prediction (Chamorro et al., 2002). The pressure and temperature conditions of BMO crystallization are much more extreme than those already tested in experiments and calculations. It is very difficult to extrapolate any bulk partition coefficient from moderate pressure values. In order to account for this range of uncertainty, the partition coefficients of He and Ne are varied by several orders of magnitude in the following models, from  $10^{-4}$  (very incompatible) to 10 (compatible).

##### 4.1. Helium and trace element concentrations

The Helium budget of a primitive-like mantle plume is mostly made from a mixture of convecting mantle and entrained pile material. The concentration of Helium in the convecting mantle has evolved through degassing at the surface, leaving less than 1% of its primordial content. The concentration of Helium in pile material is set by a two-stage process: (1) the formation of the BMO involves partitioning and noble gases dissolution into the magma and (2) crystallization of the BMO which fractionates noble gases between the melt and the solids. If Helium is incompatible, the first stage enriches the BMO compared to the mantle while the second stage generates depleted crystals. However, since crystallization is fractional the BMO becomes more and more concentrated in Helium and the crystals become enriched compared to the degassed mantle. The more incompatible Helium is, the later this situation occurs. If the crystals are enriched soon enough, the average concentration in piles can be higher than that of the degassed bulk mantle. This configuration happens if  $D_{He} > 0.01$  as seen in Fig. 3.

The evolution of pile concentration for any trace element can be described by the same dynamical model presented above, taking the HP–HT partition coefficients from Corgne et al. (2005). These experiments have been conducted at 25 GPa, the top of the lower mantle, but they represent the only available data set. As seen in Fig. 4,

**Table 1**  
Concentrations and parameters used for the bulk mantle before BMO and continental crust formation used in the model.

| Parameter   | Value  |
|---|--|
| Initial concentrations for trace elements         | given in Sun and McDonough (1995)                    |
| Th/U  | 4  |
| Initial $^3\text{He}$                             | $0.04\text{--}4 \times 10^{-9}$ mol $\text{kg}^{-1}$ |
| Initial $^4\text{He}/^3\text{He}$                 | 2500   |
| Initial $^{21}\text{Ne}/^{22}\text{Ne}$           | 0.03118 (Trieloff and Kunz, 2005)                    |
| Initial $^{22}\text{Ne}/^3\text{He}$              | 1  |
| Partition coefficients of trace elements at HT–HP | given in Corgne et al. (Corgne et al., 2005)         |
| DU  | 0.03 (Corgne et al., 2005)                           |
| DTh   | 0.005 (Corgne et al., 2005)                          |
| Initial mass of the BMO                           | $0.78 \times 10^{24}$ kg                             |
| Present day mass of the piles                     | $0.22 \times 10^{24}$ kg                             |
| Decay time of the BMO                             | 890 Ma   |
| Starting age for pile stabilization               | 4.0–3.0 Ga   |

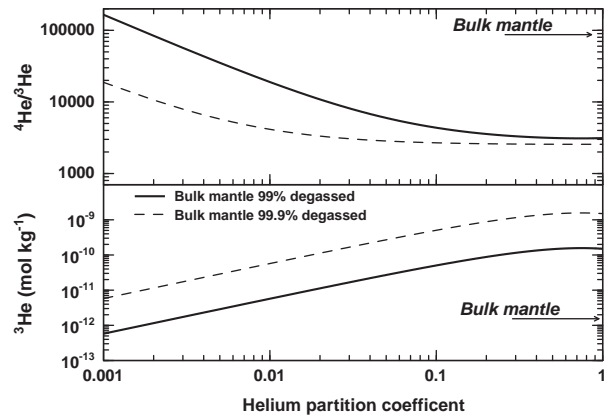


**Fig. 3.** Computed dependence of Helium concentration and  $^4\text{He}/^3\text{He}$  in the piles (for present-day) formed from crystallization of the BMO, as a function of the partition coefficient of Helium. The composition of the bulk mantle used in our calculation is compared to that of the piles. Slightly incompatible behavior of He leads to gas-rich and primitive-like pile material.

the magnitude of the concentration of some trace elements in the stable crystallized piles is close to the bulk mantle (but some elemental ratios like Th/U could significantly differ). This is in contrast to Helium, which can be 100 times richer than the bulk mantle if it is moderately incompatible at HP–HT. Continuous and intense degassing reduces the bulk mantle noble gas concentration by a factor of 10 to 1000, while silicate differentiation only reduces the concentration of incompatible trace elements by a factor of 10 or less. If  $D_{He} > 0.01$ , pile material is enriched in Helium while depleted in most of the incompatible trace elements. To explain the noble gases, the BMO model requires  $D_{He} > 0.01$ .

##### 4.2. $^4\text{He}/^3\text{He}$ in plumes

The concentration of Helium in pile material and  $^4\text{He}/^3\text{He}$  is strongly anti-correlated for  $D_{He} < D_U$  as shown in Fig. 3. Indeed, if He is more incompatible than U, Helium remains trapped in the BMO while U is extracted more efficiently toward the pile where radiogenic ingrowth contributes to increased  $^4\text{He}/^3\text{He}$ . However,  $^4\text{He}/^3\text{He}$  is not

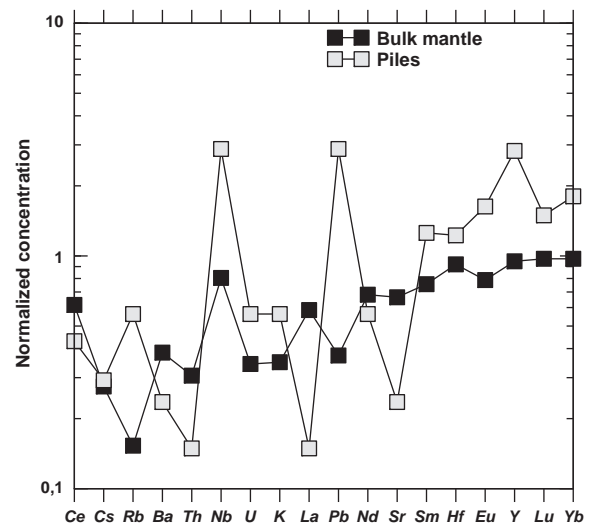


**Fig. 4.** Predicted present-day concentration within the crystallized piles for some incompatible elements (computed in this study) and bulk mantle (see Labrosse et al., 2007). The concentrations are normalized by the primitive mantle composition of McDonough and Sun (1995).

very sensitive to  $D_{He}/D_U$  as long as  $D_{He} \geq D_U$ . In this case, the signal is dominated by the concentration of  $^3He$  in piles and the isotopic ratio is close to the unfractiated value of 2000.

The isotopic ratio observed in a hotspot basalt reflects a mixing between several sources. In the case of a binary mixing of bulk mantle material and pile material, low  $^4He/^3He$  can be obtained as long as  $D_{He}$  is larger than 0.01 as seen in Fig. 5. The higher the contribution of pile material, the lower  $^4He/^3He$  can be: less than 10% of pile in the plume is sufficient to produce the  $^4He/^3He$  observed in the most primitive-like hotspots. We obtained similar results for Neon. This is because (1) pile material has a higher concentration than the bulk mantle and (2) the isotopic difference between piles and bulk mantle is more than 95%.

For refractory elements, less than 10% of pile material has a much smaller impact on the isotopic ratios of plumes. The abundances are similar to that of the bulk mantle, hence the budget is dominated by that of the latter. Because parent–daughter fractionation for these systems is limited (compared to noble gas systems where the daughter is lost in gas phases), the isotopic variations can rarely intrinsically exceed 10%. As a consequence, the contamination of pile material in the plume source does not generate significant isotopic anomalies for refractory elements while it does for noble gasses as long as they are compatible to moderately incompatible.

### 4.3. Helium vs. Neon

A substantial dataset of measurements of Neon and Helium ratios from mantle-derived samples has been built over the years. It is now clear that  $^{21}Ne/^{22}Ne$  and  $^4He/^3He$  ratios are correlated in MORBs and OIB (Hopp and Trierloff, 2008; Kurz et al., 2009; Moreira et al., 1995; Moreira et al., 2004; Moreira and Allègre, 1998). The fact that a majority of MORB and OIB samples fall on the same mixing hyperbola suggest that the mantle has only two components for the rare gasses that experienced different degrees of elemental fractionation (see the detailed study of Hopp and Trierloff, 2008). Here we propose that these two components are bulk mantle material and pile material. The other information derived from the hyperbola is that the  $^3He/^{22}Ne$  ratio is different in these two components. There is a factor of ~5–10 difference between these two ratios. The origin of this difference is not yet explained, although mantle degassing can contribute if Ne is less soluble in melt than He. A consequence of the concavity of the hyperbola is that a small amount of pile material having a low  $^3He/^{22}Ne$  changes the isotopic composition of Neon more than that of the Helium.

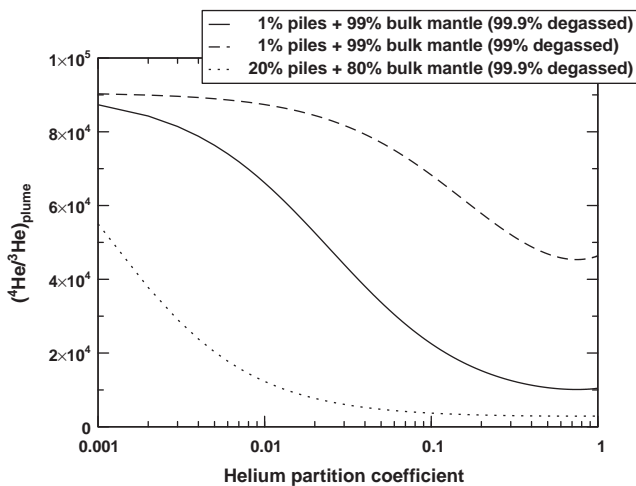


Fig. 5. Dependence of  $^4He/^3He$  in plume material on  $D_{He}$  and entrained fraction of crystals. The plume is composed of a mixing between pile material and ambient degassed mantle.

Because the isotopic ratios in piles are mostly set by the melt–crystal partition coefficients at HP–HT, the covariation of  $^{21}Ne/^{22}Ne$  and  $^4He/^3He$  constitutes a constraint on the relative partitioning of He and Ne. We compute the Ne and He composition of mixtures of pile and bulk mantle material, varying the partition coefficients of He and Ne. The composition of the bulk mantle is determined from the composition of natural samples,  $^4He/^3He$ ,  $^{21}Ne/^{22}Ne$  and  $^3He/^{22}Ne$  being 90,000, 0.06 and 5 respectively (Moreira and Allègre, 1998). To compute the pile component we use a primordial concentration for  $^3He$  which is 1000 times that of the present-day degassed mantle. The range of partition coefficients follows the results detailed in the previous section in order to reproduce the extreme values in plume material. In Fig. 6, the dataset is shown along with model predictions for different  $D_{Ne}/D_{He}$  fixing  $D_{He}=0.01$ . The hyperbola depicted in Fig. 6 shows that the most primitive-like oceanic island basalts require less than 10% of pile material in their source as we proposed above. The distribution of the data is well fitted by a mixture of pile material and bulk mantle material for  $D_{Ne}/D_{He}$  larger than, but very close to, a value of unity. Our model suggests that Helium and Neon have the same incompatible element behavior at high pressure and little BMO fractionation between them is needed in our model. In comparison, subsurface fractionation is more effective since the  $^3He/^{22}Ne$  of the bulk mantle increased from 1 (initial value) to 5 (present-day value).

### 5. Discussion and conclusions

Fractionation caused by crystallization in the deepest mantle has a chemical expression in mantle evolution through the generation of two anomalous reservoirs: the BMO and the dense chemical piles. As explained in Labrosse et al. (2007), the BMO has large density and rheology contrasts with the overlying solid mantle that make this reservoir stable and preserved from immediate entrainment. The formation of an isolated reservoir early in Earth’s history has been also proposed by Boyet and Carlson (2006). Cooling of the mantle modifies the BMO by extracting crystals hence reducing its volume. The crystals that can be remixed back into the overlying convecting mantle record the crystallization history of the BMO. For this reason they have a chemical signature distinct from the bulk mantle. Relatively early in the history of the Earth, these crystals become sufficiently rich in Fe through ongoing fractional crystallization that they can be dense enough to resist viscous entrainment and grow piles. Only plumes can transfer pile material to the surface and provide a small amount of material whose unique isotopic composition may then be measured.

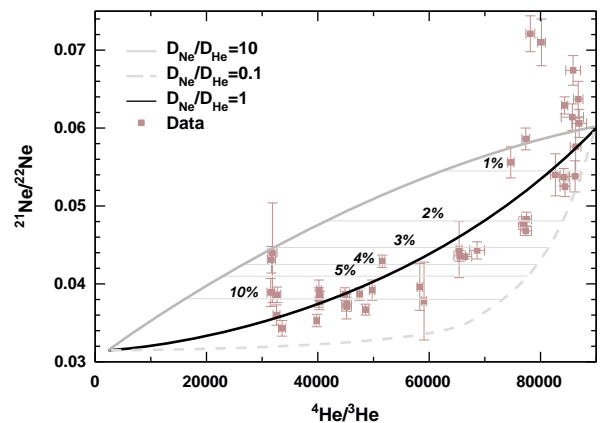


Fig. 6. Mixing hyperbola for  $^4He/^3He$  and  $^{21}Ne/^{22}Ne$  obtained with our model for different  $D_{Ne}/D_{He}$  (given that  $D_{He}$  is 0.01). The model predictions are presented along with measurements on OIBs (Kurz et al., 2005; Moreira et al., 2001, 1995; Raquin and Moreira, 2009).

We explored models of evolution of Helium and Neon isotopes in the deep mantle. The outcomes of the numerical experiments depend mostly on the partitioning of Helium and Neon. The primitive-like signature of some OIBs can be explained by the presence of limited amounts of pile material (<10%) in the plume source if the partition coefficients of Helium and Neon are larger than 0.01 and their ratio close to 1. Only low pressure experiments have been conducted to investigate the partitioning behavior of He and Ne between melt and silicates. A recent and extensive study by Heber et al. (2007) suggests a very incompatible behavior of He and Ne at low pressure for melting of olivine and clinopyroxene ( $D \sim 10^{-4}$ ). In these experiments the ratios of the partition coefficients of He and Ne are close to one, slightly lower for olivine while slightly larger for clinopyroxene. Because the ratio remains similar, the mechanism of the increase of compatibility is probably similar for both elements. A theoretical study on melt structures shows that the structure of liquid and solid becomes more similar as one goes to higher pressure along the melting curve (Stixrude et al., 2009). As a consequence noble gasses and other elements could become more compatible at very high pressure.

The small amount of pile material needed in the model agrees with the geochemistry of refractory elements in plumes. Indeed, one of the difficulties for explaining the peculiar noble gas data is that no associated correlation with refractory elements is observed. Primitive-like plumes have depleted Pb, Nd, Sr signatures, that sometimes are close to that of the depleted mantle. For Hawaii or Iceland, only Helium, Neon and Argon display anomalies in their source relative to MORBs. We have shown that through degassing, variation in concentrations can be several orders of magnitude (easily a factor of 100 or more) and differences in isotopic ratios can be a factor of 10. For refractory elements, differentiation through BMO evolution generates smaller concentration variations, and isotopic differences in Pb, Sr or Nd that are intrinsically too small to make a difference given a limited amount of entrained pile material. For these reasons, incorporating a small amount of pile material can modify strongly the noble gas signature in plumes while leaving the refractory element/isotope budget mostly undisturbed. Hence, our model proposes noble gasses and refractory elements would carry a different message (BMO vs. recycling). This prediction has to be investigated since the relationship between noble gas and refractory isotope is the subject of an ongoing debate (Class and Goldstein, 2005; Graham, 2002; Hanan and Graham, 1996; Jackson et al., 2010; Mukhopadhyay et al., 2003).

## Acknowledgments

This work is supported by Agence Nationale de la Recherche (DynBMO, ANR-08-JCJC-0084-01) and by the National Science Foundation (NSFEAR0855737). We thank the constructive and careful reviews of J. Hopp and S. Mukhopadhyay, as well as the editorship of R. Carlson.

## References

- Albarède, F., 2009. Volatile accretion history of the terrestrial planets and dynamic implications. *Nature* 461, 1227–1233. doi: 10.1038/nature08477.
- Allègre, C.J., Staudacher, T., Sarda, P., 1987. Rare-gas systematics – formation of the atmosphere, evolution and structure of the Earth's mantle. *Earth Planet Sci. Lett.* 81, 127–150.
- Ballentine, C., Marty, B., Lollar, B., Cassidy, M., 2005. Neon isotopes constrain convection and volatile origin in the Earth's mantle. *Nature* 433, 33–38. doi: 10.1038/nature03182.
- Bennett, V., Brandon, A., Nutman, A., 2007. 142Nd–143Nd isotopic evidence for Hadean mantle dynamics. *Science* 318, 1907–1910. doi: 10.1126/science.1145928.
- Black, D., 1971. Trapped neon–argon isotopic correlations in gas rich meteorites and carbonaceous chondrites. *Geochim. Cosmochim. Acta* 35, 230–235.
- Blichert-Toft, J., Frey, F., Albarède, F., 1999. Hf isotope evidence for pelagic sediments in the source of hawaiian basalts. *Science* 285, 879–882.
- Bolton, H., Masters, G., 2001. Travel times of P and S from the global digital seismic networks: implications for the relative variation of P and S velocity in the mantle. *J. Geophys. Res.* 106, 13527–13540.
- Boyet, M., Carlson, R., 2006. A new geochemical model for the Earth's mantle inferred from 146Sm–142Nd systematics. *Earth Planet Sci. Lett.* 250, 254–268. doi: 10.1016/j.epsl.2006.07.046.
- Brooker, R., Du, Z., Blundy, J., Kelley, S., Allan, N., Wood, B., Chamorro, E., Wartho, J., Purton, J., 2003. The 'zero charge' partitioning behaviour of noble gases during mantle melting. *Nature* 423, 738–741. doi: 10.1038/nature01708.
- Chamorro, E., Brooker, R., Wartho, J., Wood, B., Kelley, S., Blundy, J., 2002. Ar and K partitioning between clinopyroxene and silicate melt to 8 GPa. *Geochim. Cosmochim. Acta* 66, 507–519.
- Class, C., Goldstein, S., 2005. Evolution of helium isotopes in the Earth's mantle. *Nature* 436, 1107–1112. doi: 10.1038/nature03930.
- Coltice, N., Marty, B., Yokochi, R., 2009. Xenon isotope constraints on the thermal evolution of the early Earth. *Chem. Geol.* 266, 4–9. doi: 10.1016/j.chemgeo.2009.04.017.
- Coltice, N., Ricard, Y., 1999. Geochemical observations and one layer mantle convection. *Earth Planet Sci. Lett.* 174, 125–137.
- Coltice, N., Ricard, Y., 2002. On the origin of noble gases in mantle plumes. *Phil. Trans. R. Soc. Lond. A* 360, 2633–2648. doi: 10.1098/rsta.2002.1084.
- Corgne, A., Liebske, C., Wood, B., Rubie, D., Frost, D., 2005. Silicate perovskite–melt partitioning of trace elements and geochemical signature of a deep perovskitic reservoir. *Geochim. Cosmochim. Acta* 69, 485–496. doi: 10.1016/j.gca.2004.06.041.
- Davaille, A., 1999. Simultaneous generation of hotspots and superswells by convection in a heterogeneous planetary mantle. *Nature* 402, 756–760.
- Dupré, B., Allègre, C., 1983. Pb–Sr isotope variation in Indian-ocean basalts and mixing phenomena. *Nature* 303, 142–146.
- Fiquet, G., Auzende, A.L., Siebert, J., Corgne, A., Bureau, H., Ozawa, H., Garbarino, G., 2010. Melting of peridotite to 140 gigapascals. *Science* 329, 1516–1518. doi: 10.1126/science.1192448.
- Graham, D., 2002. Noble gas isotope geochemistry of mid-ocean ridge and ocean island basalts: characterization of mantle source reservoirs. In: Porcelli, D., Ballentine, C.J., Wieler, R. (Eds.), *Noble Gases in Geochemistry and Cosmochemistry: Reviews in Mineralogy & Geochemistry*, vol. 47, pp. 247–317. AUG, 2002.
- Grimberg, A., Baur, H., Bochsler, P., Buehler, F., Burnett, D., Hays, C.C., Heber, V.S., Jurewicz, A., Wieler, R., 2006. Solar wind neon from genesis: implications for the lunar noble gas record. *Science* 314, 1133–1135. doi: 10.1126/science.1133568.
- Hanan, B., Graham, D., 1996. Lead and helium isotope evidence from oceanic basalts for a common deep source of mantle plumes. *Science* 272, 1573.
- Hart, S., 1988. Heterogeneous mantle domains – signatures, genesis and mixing chronologies. *Earth Planet Sci. Lett.* 90, 273–296.
- Hauri, E., Hart, S., 1993. Re–Os isotope systematics of HIMU and EMII oceanic island basalts from the south-Pacific ocean. *Earth Planet Sci. Lett.* 114, 353–371.
- Heber, V., Brooker, R., Kelley, S., Wood, B., 2007. Crystal–melt partitioning of noble gases (helium, neon, argon, krypton, and xenon) for olivine and clinopyroxene. *Geochim. Cosmochim. Acta* 71, 1041–1061. doi: 10.1016/j.gca.2006.11.010.
- Hernlund, J., Houser, C., 2008. The statistical distribution of seismic velocities in Earth's deep mantle. *Earth Planet Sci. Lett.* 265, 423–437. doi: 10.1016/j.epsl.2007.10.042.
- Hofmann, A., 1997. Mantle geochemistry: the message from oceanic volcanism. *Nature* 385, 219–229.
- Honda, M., McDougall, I., Patterson, D., Doulgeris, A., Clague, D., 1991. Possible solar noble-gas component in Hawaiian basalts. *Nature* 349, 149–151.
- Hopp, J., Trierloff, M., 2008. Helium Deficit in High-He-3/He-4 Parent Magmas: Predegassing Fractionation, Not a "Helium Paradox". doi: 10.1029/2007GC001833. G3 9.
- Jackson, M., Carlson, R., Kurz, M., Kempton, P., Francis, D., Blusztajn, J., 2010. Evidence for the survival of the oldest terrestrial mantle reservoir. *Nature* 466. doi: 10.1038/nature09287 853–U84.
- Karason, H., van der Hilst, R., 2001. Tomographic imaging of the lowermost mantle with differential times of refracted and diffracted core phases (PKP, P-diff). *J. Geophys. Res.* 106, 6569–6587.
- Karki, B., Stixrude, L., 2010. Viscosity of MgSiO<sub>3</sub> liquid at Earth's mantle conditions: implications for an early magma ocean. *Science* 328, 740–742.
- Kurz, M., Curtice, J., Fornari, D., Geist, D., Moreira, M., 2009. Primitive neon from the center of the Galapagos hotspot. *Earth Planet Sci. Lett.* 286, 23–34. doi: 10.1016/j.epsl.2009.06.008.
- Kurz, M., Moreira, M., Curtice, J., Lott, D., Mahoney, J., Sinton, J., 2005. Correlated helium, neon, and melt production on the super-fast spreading East Pacific Rise near 17 degrees S. *Earth Planet Sci. Lett.* 232, 125–142. doi: 10.1016/j.epsl.2005.01.005.
- Labrosse, S., 2003. Thermal and magnetic evolution of the Earth's core. *Phys. Earth Planet Inter.* 140, 127–143. doi: 10.1016/j.pepi.2003.07.006.
- Labrosse, S., Hernlund, J., Coltice, N., 2007. A crystallizing dense magma ocean at the base of the Earth's mantle. *Nature* 450, 866–869. doi: 10.1038/nature06355.
- McDonough, W., Sun, S., 1995. The composition of the Earth. *Chem. Geol.* 120, 223–253.
- McNamara, A., Garnero, E., Rost, S., 2010. Tracking deep mantle reservoirs with ultra-low velocity zones. *Earth Planet Sci. Lett.* 437, 1–9.
- McNamara, A., Zhong, S., 2005. Thermochemical structures beneath Africa and the Pacific Ocean. *Nature* 437, 1136–1139. doi: 10.1038/nature04066.
- Megnini, C., Romanowicz, B., 2000. The three-dimensional shear velocity structure of the mantle from the inversion of body, surface and higher-mode waveforms. *Geophys. J. Int.* 143, 709–728.
- Moreira, M., Allègre, C., 1998. Helium–neon systematics and the structure of the mantle. *Chem. Geol.* 147, 53–59.
- Moreira, M., Breddam, K., Curtice, J., Kurz, M., 2001. Solar neon in the Icelandic mantle: new evidence for an undegassed lower mantle. *Earth Planet Sci. Lett.* 185, 15–23.
- Moreira, M., Doucet, S., Madureira, P., Lecomte, A., Allègre, C., 2004. Helium–Neon systematics in OIB and the nature of the source of mantle plumes. *Geochim. Cosmochim. Acta* 68, A283.

- Moreira, M., Staudacher, T., Sarda, P., Schilling, J., Allègre, C., 1995. A primitive plume neon component in MORB – the Shona ridge-anomaly, south-atlantic (51–52-degrees-S). *Earth Planet Sci. Lett.* 133, 367–377.
- Mosenfelder, J., Asimow, P., Ahrens, T., 2007. Thermodynamic properties of Mg<sub>2</sub>SiO<sub>4</sub> liquid at ultra-high pressures from shock measurements to 200 GPa on forsterite and wadsleyite. *J. Geophys. Res.* 112. doi: 10.1029/2006JB004364.
- Mosenfelder, J., Asimow, P., Frost, D., Rubie, D., Ahrens, T., 2009. The MgSiO<sub>3</sub> system at high pressure: thermodynamic properties of perovskite, postperovskite, and melt from global inversion of shock and static compression data. *J. Geophys. Res.* 114. doi: 10.1029/2008JB005900.
- Mukhopadhyay, S., Lassiter, J., Farley, K., Bogue, S., 2003. Geochemistry of Kauai Shield-Stage Lavas: Implications for the Chemical Evolution of the Hawaiian Plume. *Geophys. Geochem. Geosys.* 4. doi: 10.1029/2002GC000342.
- Parman, S., Kurz, M., Hart, S., Grove, T., 2005. Helium solubility in olivine and implications for high He-3/He-4 in ocean island basalts. *Nature* 437, 1140–1143. doi: 10.1038/nature04215.
- Poreda, R., Farley, K., 1992. Rare-gases in Samoan xenoliths. *Earth Planet Sci. Lett.* 113, 129–144.
- Raquin, A., Moreira, M., 2009. Atmospheric Ar-38/Ar-36 in the mantle: implications for the nature of the terrestrial parent bodies. *Earth Planet Sci. Lett.* 287, 551–558. doi: 10.1016/j.epsl.2009.09.003.
- Rost, S., Garnero, E., Williams, Q., Manga, M., 2005. Seismological constraints on a possible plume root at the core–mantle boundary. *Nature* 435, 666–669. doi: 10.1038/nature03620.
- Stixrude, L., de Koker, N., Sun, N., Mookherjee, M., Karki, B., 2009. Thermodynamics of silicate liquids in the deep Earth. *Earth Planet Sci. Lett.* 278, 226–232.
- Storey, M., Saunders, A., Tarney, J., Leat, P., Thirlwall, M., Thompson, R., Menzies, M., Marriner, G., 1988. Geochemical evidence for plume mantle interactions beneath Kerguelen and Heard Islands, Indian-Ocean. *Nature* 336, 371–374.
- Tarduno, J., Cottrell, R., Watkeys, M., Bauch, D., 2007. Geomagnetic field strength 3.2 billion years ago recorded by single silicate crystals. *Nature* 446, 657–660. doi: 10.1038/nature05667.
- Tolstikhin, I., Hofmann, A., 2005. Early crust on top of the Earth's core. *Phys. Earth Planet. Int.* 148, 109–130. doi: 10.1016/j.pepi.2004.05.011.
- Trieloff, M., Kunz, J., 2005. Isotope systematics of noble gases in the Earth's mantle: possible sources of primordial isotopes and implications for mantle structure. *Phys. Earth Planet. Inter.* 148, 13–38. doi: 10.1016/j.pepi.2004.07.007.
- Trieloff, M., Kunz, J., Allègre, C., 2002. Noble gas systematics of the Reunion mantle plume source and the origin of primordial noble gases in Earth's mantle. *Earth Planet Sci. Lett.* 200, 297–313.
- Trieloff, M., Kunz, J., Clague, D., Harrison, D., Allègre, C., 2000. The nature of pristine noble gases in mantle plumes. *Science* 288, 1036–1038.
- Wieler, R., 2002. Noble gases in the solar system. In: Porcelli, D., Ballentine, C., Wieler, R. (Eds.), *Noble Gases in Geochemistry and Cosmochemistry: Reviews in Mineralogy & Geochemistry*, vol.47, pp. 21–70. 2002.
- Williams, Q., Garnero, E., 1996. Seismic evidence for partial melt at the base of Earth's mantle. *Science* 273, 1528–1530.
- Wood, B., Blundy, J., 2001. The effect of cation charge on crystal–melt partitioning of trace elements. *Earth Planet Sci. Lett.* 188, 59–71.
- Yokochi, R., Marty, B., 2004. A determination of the neon isotopic composition of the deep mantle. *Earth Planet Sci. Lett.* 225, 77–88. doi: 10.1016/j.epsl.2004.06.010.